Published in final edited form as:
Eur J Inorg Chem. 2012 September ; 2012(27): . doi:10.1002/ejic.201200599.

Synthesis and characterization of *fac*-Re(CO)$_3$-aspartic-*N*-monoacetic acid, a structural analogue of a potential new renal tracer, *fac*-^{99m}Tc(CO)$_3$(ASMA)

Jeffrey Klenc[a], **Malgorzata Lipowska**[a,*], **Andrew T. Taylor**[a], and **Luigi G. Marzilli**[b]

[a]Department of Radiology and Imaging Sciences, Emory University, 1364 Clifton Rd, Atlanta, GA 30322, USA

[b]Department of Chemistry, Louisiana State University, Baton Rouge, LA 70803, USA

Abstract

The reaction of an aminopolycarboxylate ligand, **as**partic-*N*-**m**onoacetic **a**cid (ASMA), with $[Re(CO)_3(H_2O)_3]^+$ was examined. The tridentate coordination of ASMA to this Re^I tricarbonyl precursor yielded *fac*-Re(CO)$_3$(ASMA) as a mixture of diastereomers. The chemistry is analogous to that of the Tc^I tricarbonyl complex, which yields *fac*-^{99m}Tc(CO)$_3$(ASMA) under similar conditions. The formation, structure, and isomerization of *fac*-Re(CO)$_3$(ASMA) products were characterized by HPLC, ^{1}H NMR spectroscopy, and X-ray crystallography. The two major *fac*-Re(CO)$_3$(ASMA) diastereomeric products each have a linear ONO coordination mode with two adjacent five-membered chelate rings, but they differ in the endo or exo orientation of the uncoordinated acetate group, in agreement with expectations based on previous studies. Conditions have been identified for the expedient isomerization of *fac*-Re(CO)$_3$(ASMA) to a mixture consisting primarily of one major product. Because different isomeric species typically have different pharmacokinetic characteristics, these conditions may provide for the practical isolation of a single ^{99m}Tc(CO)$_3$(ASMA) species, thus allowing the isolation of the isomer that has optimal imaging and pharmacokinetic characteristics. This information will aid in the design of future ^{99m}Tc radiopharmaceuticals.

Keywords

Rhenium; Aminopolycarboxylate ligands; Ligand design; Isomer resolution; Imaging agents

Introduction

Rhenium (Re) complexes are currently being investigated for use as luminescent probes,[1] CNS agents,[2] and chemotherapy agents.[3] As a congener of Tc, Re complexes are also commonly employed as structural analogues for ^{99m}Tc radiotracers.[4] Re analogues allow for elucidation of ^{99m}Tc radiopharmaceuticals, which are otherwise difficult to characterize owing to the short half-life of ^{99m}Tc ($t_{1/2}$ = 6 h) and the tracer level conditions (no-carrier-added) of radiopharmaceutical preparations. Methods for the preparation of Re complexes have been developed to mirror standard radiolabeling conditions for various ^{99m}Tc complexes, including routes to ^{99m}Tc^V-oxo,[5] ^{99m}Tc^{III}-trioxo,[6] and ^{99m}Tc^I-tricarbonyl

*Corresponding author. Fax: 404-727-3488, mlipows@emory.edu.

Supporting information for this article is available on the WWW under http://www.eurjic.org/ or from the author.

Supporting Information (see footnote on the first page of this article): HPLC chromatograms showing the final products and their isomerization are included along with data tables for Figures 3 and 4.

complexes.[7] The recently improved preparation of Re^{I}-tricarbonyl complexes via the Re precursor, $[Re(CO)_3(H_2O)_3]OTf$,[8] has been especially helpful in characterizations of several new $^{99m}Tc(CO)_3^+$ renal tracers developed as potential replacements for the most widely used ^{99m}Tc renal tracer, ^{99m}TcO-mercaptoacetyltriglycine (^{99m}Tc-MAG3).[8–9]

We recently designed, prepared, and evaluated the efficacy of *fac*-$^{99m}Tc(CO)_3$(**as**partic-*N*-**m**onoacetic **a**cid), abbreviated as *fac*-$^{99m}Tc(CO)_3$(ASMA), as a potential new renal tracer.[10] *Note that we have adopted the following naming conventions which distinguish the chirality of the ligand*: "$Re(CO)_3$(ʟ-ASMA)" refers to a complex with ʟ-ASMA, whereas "$Re(CO)_3$(ASMA)" refers to a complex with any preparation of ASMA ligand. In order to simplify nomenclature, we have omitted the "*fac*-" prefix and any designation of the ligand protonation state (such as $ASMAH_3$, or ASMAH) for the remainder of this report.

We determined that the pharmacokinetic properties of $^{99m}Tc(CO)_3$(ASMA) in normal rats are comparable to those of ^{131}I-*ortho*-iodohippurate (^{131}I-OIH), the radioactive standard for measurements of effective renal plasma flow, and even superior to ^{131}I-OIH in rats with simulated renal failure.[9e, 10] Thorough structural characterization of $^{99m}Tc(CO)_3$(ASMA) is necessary because the radiotracer can exist as any of several distinct isomers. Structural ambiguity arises from several factors including the chirality of the ASMA ligand and the fact that ASMA has more donor groups (4 groups) than available coordination sites on the $^{99m}Tc(CO)_3^+$ core (3 sites). In the absence of structural data, we relied on trends in ligand chelation mode established in studies of well-characterized Re^{I}-tricarbonyl complexes with aminopolycarboxylates and other ligands in order to predict characteristics of $^{99m}Tc^{I}(CO)_3$(ASMA) such as the chelate ring size, the linear or tripodal coordination of ASMA, and the likely orientation of uncoordinated groups.[8–9, 11]

Particularly helpful for predicting the major products of $^{99m}Tc(CO)_3$(ASMA) was the strikingly similar example, $^{99m}Tc(CO)_3$(*N*-**c**arboxymethyl**m**ercapto**s**uccinic **a**cid) ($^{99m}Tc(CO)_3$(CMSA), Figure 1).[9d] Extensive characterization of its Re analogue, $Re(CO)_3$(CMSA), showed that $M(CO)_3$(CMSA) (M = ^{99m}Tc, Re) exists as a mixture of diastereomers. In each isomer, CMSA coordinates as a tridentate ligand, forming two adjacent five-membered chelate rings in a facial OSO arrangement. The $Re(CO)_3$(CMSA) diastereomers differ only in the position and orientation of the uncoordinated acetate group, designated endo- when projecting toward the face defined by the carbonyl ligands, as in Figure 1, and exo- when projecting away from the tricarbonyl face. Because ASMA and CMSA differ only at the central heteroatom (N vs. S, respectively), we expected that $M(CO)_3$(ASMA) would also exist as a mixture of diastereomers. In order to confirm this prediction, we have prepared and characterized $Re(CO)_3$(ASMA) isomers.

Results and Discussion

The synthesis of ASMA as an enantiomerically pure sample (ʟ-ASMA, **1**, or ᴅ-ASMA, **3**) and as a racemic mixture of ᴅ- and ʟ- isomers (*rac*-ASMA, **5**) has been described previously.[12] Generally, **1** and **3** were synthesized via nucleophilic substitution of bromoacetic acid by using ʟ- or ᴅ-aspartic acid as the nucleophile. The monosubstituted product was separated in good yield from unchanged starting materials, disubstituted by-products, and excess salt by cation exchange chromatography. Synthesis of **5** in acceptable yield proceeded via Michael addition of glycine to maleic acid, which eliminated the possibility of disubstituted products. An excess of maleic acid ensured that the amino acid starting material was consumed.

$Re(CO)_3$(ASMA) complexes were prepared by combining **1**, **3**, or **5** with a slight excess of the $[Re(CO)_3(H_2O)_3]^+$ precursor and maintaining a pH of 6 by using sodium hydroxide to

replicate conditions for ^{99m}Tc labeling (Figure 2). Tetramethylammonium hydroxide was also used in the synthesis of $Re(CO)_3$(*rac*-ASMA) in attempts to facilitate crystallization of the product from aqueous solution (see below). Reaction progress was monitored by HPLC at both 20 °C and 70 °C. Coordination of **1**, **3** or **5** to $[Re(CO)_3(H_2O)_3]^+$ proceeded in an identical manner, giving mixtures that differed only as expected owing to the optical activity of the ligand.

At room temperature and pH 6, the coordination reaction progressed steadily toward completion over 4 h, whereas heating at 70 °C pushed the reaction to completion within 30 min (Figure 3). According to HPLC, treatment of $[Re(CO)_3(H_2O)_3]^+$ with **1** yields two major products, **2A** and **2B**, named by their order of elution (retention times: 16.3 min and 17.6 min, respectively). Thorough analysis of the characterization has confirmed that these products are the exo- (**2A**) and endo- (**2B**) diastereomers of $Re(CO)_3$(ASMA) shown in Figure 2, Eq. 1. Intermediates observed during the reaction with relatively short retention times (4–8 min) are likely monodentate or bidentate complexes (see Supporting Information). Two minor products with a retention time of ~14 min persist at room temperature, but quickly and completely convert to the major products **2A** and **2B** after heating for 1 h. Although these intermediates could not be isolated, we believe they are $Re(CO)_3$(ASMA) isomers having one five- and one six-membered chelate ring. Previous studies demonstrate that six-membered NO chelate rings are less energetically favorable and form more slowly than five-membered chelate rings.[13] Hence we expect that complexes with both a five-membered and a six-membered NO chelate ring will be present only in small amounts and will readily convert to products with two five-membered chelate rings, as is observed.

Identical HPLC chromatograms were observed when using either **3** or **5** as the ligand. However, for $Re(CO)_3$(*rac*-ASMA), each peak now represents an enantiomeric mixture of isomers, leading to the presence of four major products in the final reaction mixture: $Re(CO)_3$(*L*-ASMA) diastereomers **2A**, **2B** and their $Re(CO)_3$(*D*-ASMA) enantiomers **4A** and **4B** (Figure 2, Eq. 2).

Figure 3a shows that over the course of 1 d at 20 °C and pH 6, the product ratio gradually shifts toward the endo isomer, **2B**. The major products were initially formed in a ratio of 3:1 (**2A**:**2B**), but after 1 d at 20 °C the ratio had shifted to 2:1, indicating that **2A** slowly isomerizes to **2B** at these conditions. Heating the reaction mixture accelerates both the formation and isomerization reactions, as evidenced by a roughly 2:1 ratio of **2A**:**2B** obtained after just 5 min at 70 °C (Figure 3b). HPLC chromatograms before and after isomerization were compared to the sample's ^{1}H NMR spectra and showed no difference in product ratios, indicating that the ratio of isomers is not significantly affected by the HPLC method. To examine this isomerization further, a small aliquot of the product mixture (after 24 h at 20 °C, pH 6, 2:1 ratio of **2A**:**2B**) was divided into six fractions. The temperature and pH of each sample was varied, and the conversion of **2A** to **2B** was followed by HPLC (Figure 4). For conditions under which the isomerization reached equilibrium quickly (70 °C, pH ≥ 7), the final ratio of **2A**:**2B** was ~1:9. The robustness of **2A** and **2B** was not examined in particular in this study, although the complexes were chemically stable over periods of up to 7 d in the various conditions used in the isomerization study. HPLC analysis of the metabolites of $^{99m}Tc(CO)_3$(ASMA) in our parallel study[9e] shows that the complex is long lived in biological systems.

From Figure 4, it is clear that both heat and pH have a distinct effect on the isomerization of the product mixture. Without the benefit of heat or elevated pH (20 °C, pH 4), the initial product ratio of 2:1 is relatively constant. However, raising the pH to 9 at 20 °C accelerates the isomerization only slightly. Similarly, heating in acidic conditions (70 °C, pH 4) is not

practical for rapid isomerization, and the products approach equilibrium only after 7 d. Thus, to promote expedient isomerization to the thermodynamic product, **2B**, heating in neutral or slightly basic conditions is required (70 °C, pH ≥ 7). Although a thorough mechanistic study of this multi-step isomerization process is beyond the scope of this project, the acceleration of the reaction as pH increases strongly indicates that the initial step is deprotonation of the NH group by hydroxide to generate a small equilibrium amount of deprotonated complex. We hypothesize that the strongly donating N-donor thereby created will favor formation of a five-coordinate, short-lived intermediate yielding two closely related intermediates with either one of the two carboxyl groups dissociated. Collapse of either intermediate to regenerate the six-coordinate complex would lead to either the endo or exo isomer, depending on the direction in which the carboxyl moves to close the chelate ring.

Identifying the kinetic isomer (**2A**) and the thermodynamic isomer (**2B**) enables the assignment of these products to a specific diastereomer. The most energetically favorable arrangement (thermodynamic isomer **2B**) will likely have the bulky dangling $–CH_2CO_2^-$ group facing away (endo) from the crowded chelate rings formed by the tridentate ASMA ligand, (Figure 5a). Similarly, the dangling carboxylate group (at pH 6) will be negatively charged and electrostatically repelled from the negatively charged inner coordination sphere center, making the endo- isomer more thermodynamically favorable. Because the thermodynamically favored product is likely to be the endo- isomer and because this isomer should be even more favored at high pH, we can make an initial structural assignment of **2B** as *endo*-$Re(CO)_3$(ASMA). Comparisons to the ^{1}H NMR spectrum and the crystal structure of $Re(CO)_3$(CMSA) support this assignment and consequently, the assignment of **2A** (and **4A**) as *exo*-$Re(CO)_3$(ASMA).

Crystallization of K[*endo*-$Re(CO)_3$(*rac*-ASMA)] was achieved from a concentrated aqueous pH 2 solution of the equilibrated product. Slow evaporation of this sample yielded small, colorless crystals as a mixture of enantiomers **2B** and **4B**, with the uncoordinated carboxyl group protonated (Figure 5a). Attempts under similar conditions and at pH 6 to obtain crystals with a more hydrophobic counterion, NMe_4[*endo*-$Re(CO)_3$(*rac*-ASMA)], or the exo- enantiomers, NMe_4[*exo*-$Re(CO)_3$(*rac*-ASMA)] or K[*exo*-$Re(CO)_3$(*rac*-ASMA)] were unsuccessful. To confirm that the crystals obtained corresponded to the thermodynamic isomer, a small crystal was dissolved and analyzed by HPLC. The only major peak corresponded to **2B** and this peak contained >95% of the trace area. X-ray structural analysis shows that the enantiomers **2B** and **4B** (**2B** presented in Figure 5a) are indeed the endo isomer, K[*endo*-$Re(CO)_3$(*rac*-ASMA)], as predicted from results for the thermodynamic product of $Re(CO)_3$(CMSA).[9a] In the pseudo-octahedral complex, the coordinated tridentate ASMA ligand is bound in a facial ONO arrangement, giving rise to two adjacent five-membered NO chelate rings. The dangling protonated carboxyl group is facing away from the triangular ONO face as expected for the endo isomer. Bond distances between donor groups and the metal core (Re1–O4, Re1–O6, Re1–N1) are consistent with previous examples for carboxyl and amino donor groups (Table 1).[8, 14] Deviations from the expected geometry occur systematically between analogous bond angles of NMe_4[*endo*-$Re(CO)_3$(CMSA)] and those of other Re^I-tricarbonyl complexes which share a similar coordination mode.[9c, 9d] The crystal structure confirms our assignment of thermodynamic isomers **2B** and **4B** as *endo*-$Re(CO)_3$(ASMA). Additional crystallographic data for both complexes can be found at http://www.ccdc.cam.ac.uk (CCDC 884591).

The explicit characterization of **2B** supports our assignment of **2A** based on isomerization between the two products. However, the structure of **2A** remains somewhat ambiguous because in addition to the expected *exo*-$Re(CO)_3$(ASMA) product (Figure 5b), isomers with the β-carboxyl group (as labeled in Figure 1) coordinated to the metal core are possible (Figure 6). In a tripodal coordination mode, the ligand will form three chelate rings (one

five-, one six-, and one seven-membered ring) with the metal core; such an arrangement has been shown to be unfavorable compared to that of **2B**.[11a] Potential isomers with ASMA bound linearly through the β-carboxyl will form two adjacent chelate rings (one five- and one six-membered ring) which, although more likely to form than tripodal isomers, are less stable and form more slowly than **2A** because of its six-membered chelate ring. Therefore, it is very unlikely that isomers with a coordinated β-carboxyl will contribute as major products to the reaction mixture of $Re(CO)_3$(ASMA). However, as noted earlier, the isomers forming adjacent five- and six-membered chelate rings are likely the minor products that readily convert to **2A** and **2B**, as observed by HPLC.

Further confirmation of the structure of **2A** is possible through ^{1}H NMR analysis. When both major products **2A** and **2B** are present in nearly equal amounts, the ^{1}H NMR spectrum is difficult to interpret owing to the similarity in peak intensity and some overlap in peaks from the two sets (Figure 7, **I**). In the equilibrated sample (as detailed above), two sets of signals in a 1:9 ratio (**2A**:**2B**) are easily distinguishable (Figure 7, **II**). Each resonance was assigned to the appropriate diastereomer by comparing the two spectra, as shown in Figure 7. Expected signals for $Re(CO)_3$(ASMA) isomers are observed in each spectrum, including an amino proton (NH), H_α, two protons from the coordinated *N*-carboxymethyl group (*exo*- and *endo*-H_{COORD}) and two H_β protons from the uncoordinated acetate group, none of which are magnetically equivalent (Table 2). Each signal shows a splitting pattern that is consistent with the predicted coordination mode.

Comparisons of the ^{1}H NMR signals of H_α, NH, and H_{COORD} of **2A** and **2B** (Figure 7; these protons are bonded to C5, N1, and C6 respectively, Figure 5) are especially helpful for confirming the structure of **2A**. Perhaps most enlightening are differences in the shielding of H_α in *endo*-$Re(CO)_3$(ASMA) and *exo*-$Re(CO)_3$(ASMA). Data from our previous work (Table 3) suggest that protons in an exo- orientation (away from the tricarbonyl face) are more shielded than those in an endo- orientation, resulting in an upfield shift in the ^{1}H NMR signal. The orientation of the uncoordinated group can be inferred from the shift of H_α, as these two groups must assume opposing orientations. The H_α signal in **2B** (3.63 ppm) is significantly upfield of the analogous signal from **2A** (4.12 ppm). Therefore, H_α of **2A** must assume the endo- orientation, as in *exo*-$Re(CO)_3$(ASMA).

The splitting pattern of the NH signals provides additional support for the structural assignment of **2A**. NH has three neighboring protons (H_α and *exo*- and *endo*-H_{COORD}) likely to contribute to splitting of its ^{1}H NMR signal. In each diastereomer (**2A** and **2B**), the NH proton is in an endo- orientation, allowing for straightforward comparisons of signal splitting owing to the relative spatial arrangement of neighboring protons. As we observed earlier, the orientation of H_α is opposite to that of the uncoordinated acetate group. Thus, the NH signal in *endo*-$Re(CO)_3$(ASMA) (**2B**) can be split by *exo*-H_α, *exo*-H_{COORD} and *endo*-H_{COORD} (see Figure 5), whereas the NH signal in *exo*-$Re(CO)_3$(ASMA) can be split by *endo*-H_α, *exo*-H_{COORD} and *endo*-H_{COORD}. This difference is significant because, according to the crystal structure of **2B**, both *exo*-H_{COORD} and *exo*-H_α protons in **2B** have torsion angles near 90° with NH (*exo*-H_{COORD}–C6–N1–H = 94.3° and *exo*-H_α–C5–N1–H = 89.3°), resulting in a coupling constant of essentially zero (Figure 5a). Consequently, in **2B** only coupling between NH and *endo*-H_{COORD} is observed, resulting in a distinct doublet at 6.18 ppm. For *exo*-$Re(CO)_3$(ASMA), we expect to see NH splitting from both *endo*-H_α and *endo*-H_{COORD} and assume that splitting from *exo*-H_{COORD} is not observed because of a nearly orthogonal torsion angle with NH, similar to that observed in **2B**. The NH splitting in **2A** matches this expectation and resembles a triplet (6.42 ppm), suggesting that the coupling constants with H_α and *endo*-H_{COORD} are similar, and allowing us to confirm the assignment of **2A** (and **4A**) as *exo*-$Re(CO)_3$(ASMA).

In addition, we expect the uncoordinated acetate group to shield the adjacent amine proton (NH) relative to its spatial proximity. In *endo*-$Re(CO)_3$(ASMA) (see crystal structure of **2B** in Figure 5a), the uncoordinated CH_2CO_2H group will be closer to the amino proton, causing the NH signal to be more shielded and hence shifting the resulting ^1H NMR signal upfield (6.18 ppm) relative to the analogous NH signal (6.42 ppm) arising from *exo*-$Re(CO)_3$(ASMA) (Table 2).

Conclusions

We have prepared $Re(CO)_3$(ASMA) as an analogue of a potential new renal tracer, $^{99m}Tc(CO)_3$(ASMA), through methods that mimic $^{99m}Tc(CO)_3^+$ labeling procedures. We demonstrated by following the reaction progress that the major products formed are analogous to those observed during the preparation of $^{99m}Tc(CO)_3$(ASMA). As predicted on the basis of previously characterized $M(CO)_3^+$ complexes, the major isomers of $M(CO)_3$(ASMA) have a facial, tridentate, ONO coordination mode with ASMA, forming two adjacent five-membered chelate rings. Coordination of either L-ASMA or D-ASMA yields a mixture of two diastereomeric complexes differing only in the position and orientation of the uncoordinated acetate group ($-CH_2CO_2^-$) on the aspartate chelate ring. The detailed characterization of $Re(CO)_3$(ASMA) isomers reinforces trends regarding the coordination of aminopolycarboxylate ligands to the M^I-tricarbonyl core, such as preferred donor groups, chelate ring size, and coordination mode.

By examining the isomerization of diastereomeric products by HPLC we have identified *endo*-$Re(CO)_3$(ASMA) (**2B** or **4B**) as the thermodynamically favored product and *exo*-$Re(CO)_3$(ASMA) (**2A** or **4A**) as the kinetically favored product. We also followed the isomerization of $Re(CO)_3$(ASMA) and outlined conditions for a practical isomerization favoring the thermodynamic product in a 9:1 ratio. This result has proved to be useful in NMR studies and in obtaining X-ray quality crystals. Because different isomeric species typically have different pharmacokinetic characteristics, the ability to control the endo/exo ratio may provide for the approximate isolation of a single $^{99m}Tc(CO)_3$(ASMA) species, thus enhancing the effect of the isomer with optimal imaging and pharmacokinetic characteristics. In addition, the characterization of $^{99m}Tc(CO)_3$(ASMA) through Re analogues will allow for subsequent evaluations of pharmacokinetic properties to be correlated to its structural features, helping to guide the design of potential new ^{99m}Tc radiopharmaceuticals.

Experimental Section

General Procedures

All reagents and solvents were purchased as reagent grade and used without further purification. Aspartic-*N*-monoacetic acid (ASMA) was synthesized as previously reported as both the racemic mixture[12e] and the optically active L-isomer,[12a] briefly described below. Triaquatricarbonyl-rhenium(I) trifluoromethanesulfonate was prepared as previously reported and used as a 0.1 M stock solution.[8] Gel filtration was performed over Sephadex G-15 beads, eluting with deionized water at a rate of 0.5 mL/min. Ion exchange chromatography was performed using Dowex 50WX4 resin, in the H^+ form. The products were washed with water, then eluted with 0.5 M NH_4OH. ^1H NMR spectra were obtained at room temperature in deuterium oxide, on a 400 MHz Varian NMR spectrometer. All chemical shifts were referenced to the water peak in D_2O (4.80 ppm). HRMS was measured by the Emory University Mass Spectrometry Center by using a Thermo Finnigan LTQ-FTMS. HPLC analyses were performed on a Waters Breeze system equipped with a Waters 2487 dual wavelength absorbance detector, Waters 1525 binary pump, and XTerra MS C18 column (5 μm; 4.6 × 250 mm), using a flow rate of 1 mL/min gradient method described

previously, with aqueous 0.05 M triethylammonium phosphate buffer, pH 2.5, as solvent A and methanol as solvent B.[9a] Elemental analyses were performed by Atlantic Microlabs, Atlanta, GA. Optical rotation was measured at 589 nm on a Perkin Elmer 541 polarimeter.

L-(*N*-carboxymethyl)aspartic acid (1, L-ASMA)

L-ASMA (**1**) was prepared as previously reported.[12a] Briefly, (*L*)-aspartic acid (0.13 g, 1.0 mmol) and bromoacetic acid (0.14 g, 1.0 mmol) were neutralized separately in water with 1 M NaOH (2 mL, 2.0 mmol) and combined. The resulting solution (10 mL) was heated to 70 °. The pH was maintained at 11 by frequent addition of 1 M NaOH, totaling 4.0 mL. No base was added after 1 h, and the solution was heated an additional 2 h without any change in the pH. The pH was adjusted to 2 by using concentrated HCl, and any salt that crystallized was removed by filtration. The crude product was purified by ion exchange chromatography to yield **1** (0.127 g, 66%) as a colorless oil. ^{1}H NMR[12a] and optical rotation[12b] data matched those of the previously reported compound. ^{1}H NMR (D_2O, pH 4) δ 3.89 (dd, 1H, *J*=3.2, 4.4 Hz); 3.72 (d, 1H, *J*=10.8 Hz); 3.64 (d, 1H, *J*=10.8 Hz); 2.91 (dd, 1H, *J*=3.2, 12.0 Hz); 2.85 (dd, 1H, *J*=4.4, 12.0 Hz). ^{13}C NMR (D_2O, pH 2) δ 37.5, 51.6, 61.3, 173.9, 175.3, 177.6. $[\alpha]_D^{20} = +4.0^\circ$ (c 1.0, H_2O). HRMS (ESI): Calcd m/z for $C_6H_{10}O_6N$ (M+), 192.05026; found, 192.05003 (Δ = −0.23 mmu, −1.22 ppm).

Re(CO)$_3$(L-ASMA) (2)

An aqueous solution of L-ASMA (0.020 g, 0.1 mmol, 5 mL) was neutralized with 1 M NaOH (0.1 mL, 0.1 mmol) and added to a stirred solution of $[Re(CO)_3(H_2O)_3]OTf$ (0.1 mmol, 0.1 M, 1.0 mL). The reaction mixture was heated at 70 °C for 30 min. Aqueous NaOH was added as needed to maintain the pH at 6. HPLC analysis of the reaction mixture revealed two peaks having retention times of 16.3 min (**2A**) and 17.3 min (**2B**) in a 2:1 ratio. The reaction mixture was concentrated to 1 mL and the products were purified by gel filtration. The UV-active fractions were analyzed by HPLC, and those without impurity were combined and concentrated under reduced pressure to yield a white solid (0.019 g, 38%). HRMS (ESI): Calcd m/z for $C_9H_7O_9N^{187}Re$ (M-), 459.96839; found, 459.96846 (Δ = 0.07 mmu, 0.14 ppm). The ^{1}H NMR spectrum showed two sets of peaks in a roughly 1:1 ratio. The mixture of isomers was heated at 70 °C for 2 d to isomerize the mixture to favor **2B**, (**2A**:**2B**, 1:5). Differences in spectra before and after isomerization were used to determine which signals were derived from each isomer.

2A: ^{1}H NMR (D_2O, pH 6) δ 6.42 (m, 1H); 4.12 (m, 1H, *J*=5.6, 8.8 Hz); 3.55 (m, 2H); 2.78 (dd, 1H, *J*=5.6, 16.4 Hz); 2.55 (dd, 1H, *J*=8.8, 16.4 Hz).

2B: ^{1}H NMR (D_2O, pH 6): δ 6.18 (d, 1H, *J*=6.8 Hz); 3.93 (dd, 1H, *J*=6.8, 17.2 Hz); 3.67 (d, 1H, *J*=17.2 Hz); 3.63 (dd, 1H, *J*=6.0, 8.0 Hz); 2.69 (d, 1H, *J*=8.0 Hz); 2.68 (d, 1H, *J*=6.0 Hz).

D-(*N*-carboxymethyl)aspartic acid (3, D-ASMA)

D-ASMA (**3**) was prepared similarly to **1**, by using D-aspartic acid instead of L-aspartic acid. The product was purified by ion exchange chromatography to yield **3** (0.105 g, 55%) as a colorless oil. The ^{1}H NMR spectrum was identical to that of **1**. ^{1}H NMR (D_2O, pH 4) δ 3.89 (dd, 1H, *J*=3.2, 4.4 Hz); 3.72 (d, 1H, *J*=10.8 Hz); 3.64 (d, 1H, *J*=10.8 Hz); 2.91 (dd, 1H, *J*=3.2, 12.0 Hz); 2.85 (dd, 1H, *J*=4.4, 12.0 Hz). ^{13}C NMR (D_2O, pH 2) δ 37.5, 51.6, 61.3, 173.9, 175.3, 177.6. $[\alpha]_D^{20} = -10.2^\circ$ (c 1.0, H_2O). HRMS (ESI): Calcd m/z for $C_6H_{10}O_6N$ (M+), 192.05026; found, 192.05014 (Δ = −0.12 mmu, −0.64 ppm).

$Re(CO)_3$(*D*-ASMA) (4)

The reaction of *D*-ASMA (0.075 g, 0.39 mmol, 5 mL) with $[Re(CO)_3(H_2O)_3]OTf$ (0.27 mmol, 0.1 M, 2.7 mL) proceeded in an identical manner as that used to prepare **2** to yield a white solid (0.085 g, 69%). ^1H NMR spectrum was identical to that of **2**. HRMS (ESI): Calcd m/z for $C_9H_7O_9N^{187}Re$ (M-), 459.96839; found, 459.96857 (Δ = 0.18 mmu, 0.38 ppm).

(+/−)-(*N*-carboxymethyl)aspartic acid (5, *rac*-ASMA)

This compound was synthesized as previously reported.[12e] Briefly, glycine (0.075 g, 1.0 mmol) and maleic acid (0.128 g, 1.1 mmol) were combined in 10 mL of water. The pH of this mixture was adjusted to 11 with 1 M aqueous potassium hydroxide. The solution was heated near 70 °C for 1 d. The pH was adjusted to 2 with concentrated HCl and the mixture was cooled to 0 °C to precipitate KCl and starting materials. The filtrate was concentrated to yield a white solid (0.164 g) that contained some KCl. The elaborate purification method employed for **1** produced **5** (0.077 g, 40%) in high purity for ^1H NMR and HRMS analyses; however, the crude product was sufficiently pure for use in the next step. The ^1H NMR spectrum agreed with that of the previously reported compound. ^1H NMR (D_2O, pH 6) δ 3.84 (dd, 1H, *J*=4.4, 7.6 Hz); 3.70 (d, 1H, *J*=16.4 Hz); 3.64 (d, 1H, *J*=16.4 Hz); 2.83 (dd, 1H, *J*=4.0, 17.6 Hz); 2.75 (dd, 1H, *J*=7.6, 17.6 Hz). ^{13}C NMR (D_2O, pH 3) δ 37.5, 51.3, 61.7, 174.3, 175.7, 178.9. $[\alpha]_D^{20} = 0.0^\circ$ (c 1.0, H_2O). HRMS (ESI): Calcd m/z for $C_6H_8O_6N$ (M-), 190.03571; found, 190.03565 (Δ = −0.06 mmu, −0.32 ppm).

$Re(CO)_3$(*rac*-ASMA) (2 and 4)

To an aqueous solution of crude *rac*-ASMA (**5**, 0.034 M, 0.068 mmol, 2 mL) was added $NMe_4OH{\cdot}5H_2O$ (0.038 g, 0.21 mmol) and $[Re(CO)_3(H_2O)_3]OTf$ (0.068 mmol, 0.1 M, 0.68 mL), and the solution was heated at 70 °C for 30 min. HPLC analysis of the reaction mixture was identical to that of **2**, with two peaks having retention times of 16.3 min (**2A** and **4A**) and 17.3 min (**2B** and **4B**) in a ca. 2:1 ratio. The reaction mixture was concentrated to 1 mL and the products were purified by gel filtration as described above for **2** to yield the products as a white solid (0.031 g, 75%). ^1H NMR and HRMS data were identical to the data for **2** and **4**. The product was equilibrated (70 °C, pH 7, 1 d) and the endo- product was crystallized from a concentrated aqueous solution (pH 2) at room temperature as a potassium salt (the K^+ cation is present in the crude starting material, **5**).

Anal. Calcd for $C_9H_7N_9OReK$: C, 21.69; H, 1.42, N, 2.81; Found: C, 21.74; H, 1.35; N, 2.81.

Crystal structure of K[*endo*-$Re(CO)_3$(*rac*-ASMA)]

A suitable crystal was coated with Paratone N oil, suspended in a small fiber loop and placed in a cooled nitrogen gas stream at 173 K on a Bruker D8 APEX II CCD sealed tube diffractometer with graphite monochromated MoK_α (0.71073 Å) radiation. Data were measured by using a series of combinations of phi and omega scans with 10 s frame exposures and 0.5° frame widths. Data collection, indexing and initial cell refinements were all carried out with APEX II[15] software. Frame integration and final cell refinements were done by using SAINT[15] software. The final cell parameters were determined from least-squares refinement on 4395 reflections.

The structure was solved by using direct methods and difference Fourier techniques (SHELXTL, V6.12).[16] Hydrogen atoms were placed in their expected chemical positions by using the HFIX command and were included in the final cycles of least squares with isotropic U_{ij}'s related to the atoms ridden upon. All non-hydrogen atoms were refined

anisotropically. Scattering factors and anomalous dispersion corrections were taken from the *International Tables for X-ray Crystallography*.[17] Structure solution, refinement, graphics and generation of publication materials were performed by using SHELXTL, V6.12 software. These results are summarized in Table 4.

Supplementary Material

Refer to Web version on PubMed Central for supplementary material.

Acknowledgments

This work was supported by the National Institute of Health/National Institute of Diabetes and Digestive and Kidney Diseases (Grant No. R37 DK38842). The authors thank Dr. Kenneth Hardcastle of Emory University for discussions regarding crystal preparation and for the structure determination. We also thank Dr. Patricia A. Marzilli for her invaluable comments during the preparation of the paper.

References

1. Lo K, Zhang K, Li S. Eur. J. Inorg. Chem. 2011:3551–3568.
2. Louie AS, Vasdev N, Valliant JF. J. Med. Chem. 2011; 54:3360–3367. [PubMed: 21428421]
3. Fricker SP, Mosi RM, Cameron BR, Baird I, Zhu Y, Anastassov V, Cox J, Doyle PS, Hansell E, Lau G, Langille J, Olsen M, Qin L, Skerlj R, Wong RSY, Santucci Z, McKerrow JH. J. Inorg. Biochem. 2008; 102:1839–1845. [PubMed: 18684510]
4. a) García Garayoa E, Rüegg D, Bläuenstein P, Zwimpfer M, Khan I, Maes V, Blanc A, Beck-Sickinger AG, Tourwé DA, Schubiger PA. Nucl. Med. Biol. 2007; 34:17–28. [PubMed: 17210458] b) Esteves T, Xavier C, Gama S, Mendes F, Raposinho PD, Marques F, Paulo A, Pessoa JC, Rino J, Viola G, Santos I. Org. Biomol. Chem. 2010; 8:4104–4116. [PubMed: 20648265] c) Sagnou M, Benaki D, Triantis C, Tsotakos T, Psycharis V, Raptopoulou CP, Pirmettis I, Papadopoulos M, Pelecanou M. Inorg. Chem. 2011; 50:1295–1303. [PubMed: 21250638]
5. a) Abram U, Braun M, Abram S, Kirmse R, Voigt A. Dalton Trans. 1998:231–238.b) Nguyen HH, Jegathesh JJ, Maia PIdS, Deflon VM, Gust R, Bergemann S, Abram U. Inorg. Chem. 2009; 48:9356–9364. [PubMed: 19736964]
6. Toganoh M, Ikeda S, Furuta H. Chem. Commun. 2005:4589–4591.
7. Alberto R, Kyong Pak J, van Staveren D, Mundwiler S, Benny P. Pept. Sci. 2004; 76:324–333.
8. He H, Lipowska M, Xu X, Taylor AT, Carlone M, Marzilli LG. Inorg. Chem. 2005; 44:5437–5446. [PubMed: 16022542]
9. a) He H, Lipowska M, Xu X, Taylor AT, Marzilli LG. Inorg. Chem. 2007; 46:3385–3394. [PubMed: 17375908] b) Lipowska M, He H, Xu X, Taylor AT, Marzilli PA, Marzilli LG. Inorg. Chem. 2010; 49:3141–3151. [PubMed: 20201565] c) Lipowska M, Cini R, Tamasi G, Xu X, Taylor AT, Marzilli LG. Inorg. Chem. 2004; 43:7774–7783. [PubMed: 15554642] d) He H, Lipowska M, Christoforou AM, Marzilli LG, Taylor AT. Nuclear Medicine and Biology. 2007; 34:709–716. [PubMed: 17707812] e) Lipowska M, Klenc J, Marzilli LG, Taylor AT. J. Nucl. Med. 2012
10. Lipowska M, Klenc J, Malveaux E, Marzilli L, Taylor A. J. Nucl. Med. 2011; 52:103P.
11. a) He H, Morley JE, Twamley B, Groeneman RH, Bučar D-Ki, MacGillivray LR, Benny PD. Inorg. Chem. 2009; 48:10625–10634. [PubMed: 19842652] b) Makris G, Karagiorgou O, Papagiannopoulou D, Panagiotopoulou A, Raptopoulou CP, Terzis A, Psycharis V, Pelecanou M, Pirmettis I, Papadopoulos MS. Eur. J. Inorg. Chem. 2012
12. a) Snyder RV, Angelici RJ. J. Inorg. Nucl. Chem. 1973; 35:523–535.b) Korman S, Clarke HT. J. Biol. Chem. 1956; 221:133–142. [PubMed: 13345805] c) Miyazawa T. Bull. Chem. Soc. Jpn. 1980; 59:2555–2565.d) Takahashi KN. T., JP 07089913. 1995e) Hartman, JAR.; Woodbury, RP. US. 5,362,412. 1994.
13. Lipowska, M.; Taylor, AT.; Marzilli, LG. Technetium and other radiometals in chemistry and medicine. Mazzi, U.; Eckelman, WC.; Volkert, WA., editors. SGEditoriali, Padova: 2010. p. 281-284.

14. Correia JDG, Domingos Â, Santos I, Alberto R, Ortner K. Inorg. Chem. 2001; 40:5147–5151. [PubMed: 11559073]
15. Bruker APEX2, Program Suite for Crystallographic Software. Madison (USA): Bruker AXS Inc.; 2003.
16. Sheldrick GM. Acta Cryst. 2008; A64:112–122.
17. Wilson, AJC., editor. International Tables for X-ray Crystallography, Vol. C. Dordrecht: Academic Publishers; 1992.
18. Chem 3D Pro, Desktop Modelling Application Suite. Cambridge, MA: CambridgeSoft; 2010.

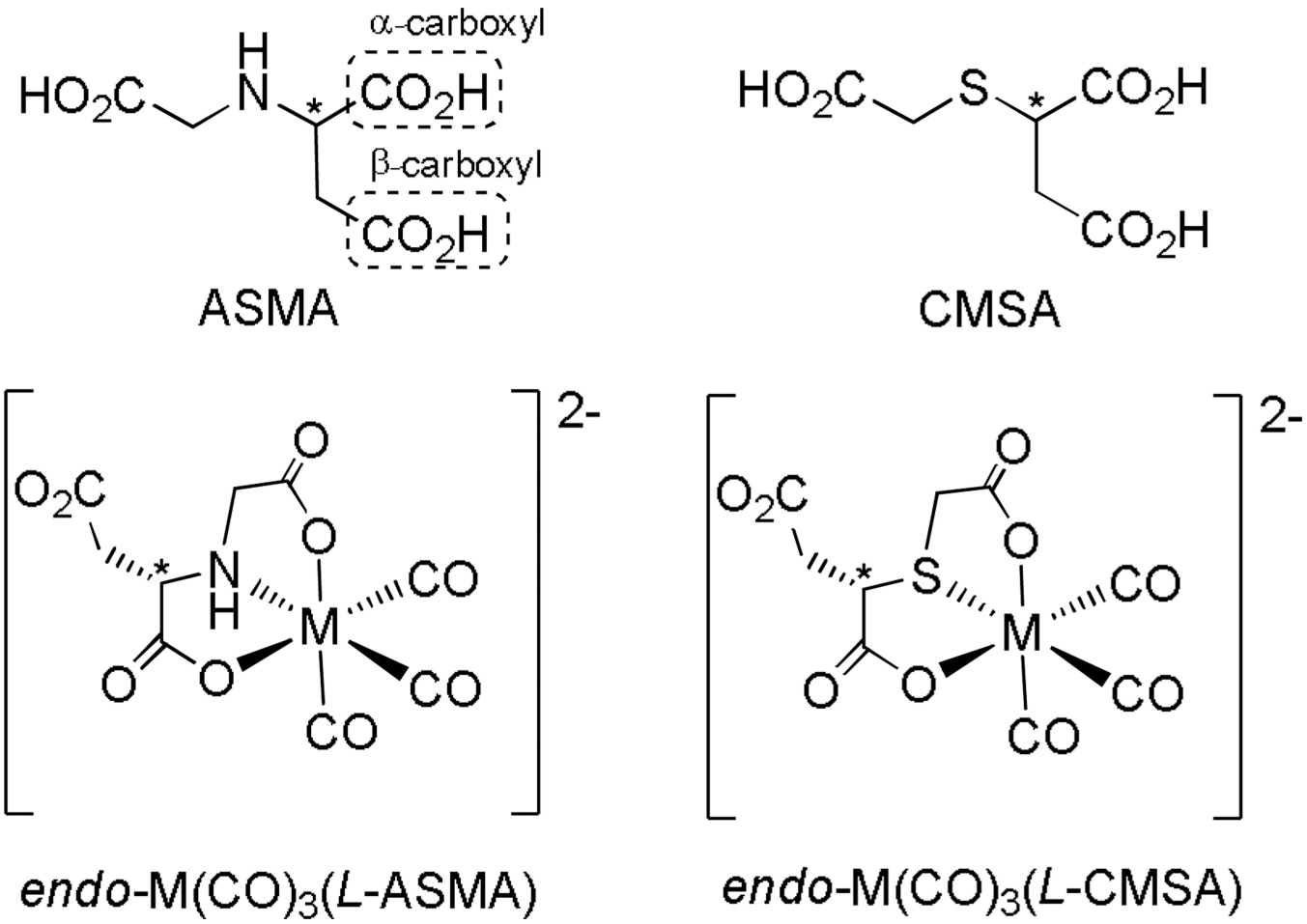

Figure 1.

Tridentate ligand chelation in $M(CO)_3$(ASMA) (M = ^{99m}Tc, Re) is expected to be similar to that in $M(CO)_3$(CMSA), yielding a diastereomeric mixture of products having an OXO (X = S, N) coordination mode with two adjacent five-membered chelate rings. Each product is expected to be dianionic near physiological pH. Only one diastereomer of each complex is shown for simplicity.

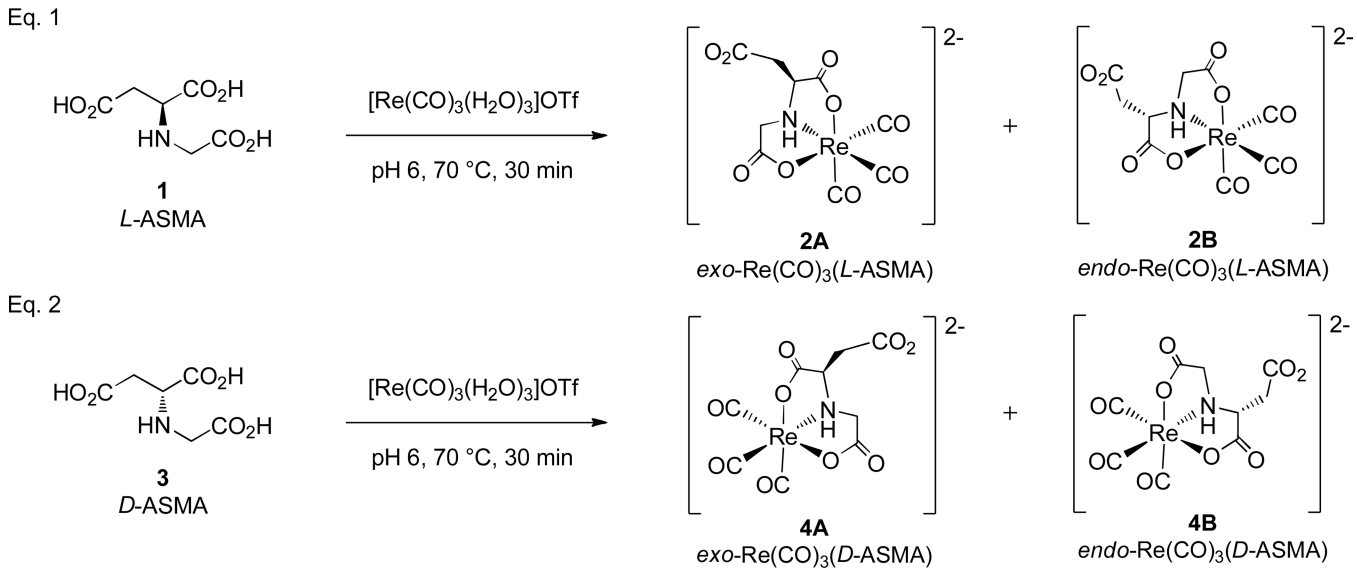

Figure 2.

Summary of coordination reactions of L-ASMA (Eq. 1) and D-ASMA (Eq. 2) with the Re^{I} tricarbonyl precursor. Each ligand gives rise to a diastereomeric mixture of products. The racemic mixture (*rac*-ASMA, **5**) gives rise to four products (two diastereomeric pairs of enantiomers **2A – 4A** and **2B – 4B**, respectively). Note that the enantiomers arise in this way because the ASMA ligand is a linear ligand with one end different from the other end. Therefore, for a facial coordination mode, isomerization between an endo- and an exo-isomer of a $M(CO)_3$(ASMA) complex for a given ASMA isomer (L or D) by necessity changes the chirality at the metal center, as illustrated above.

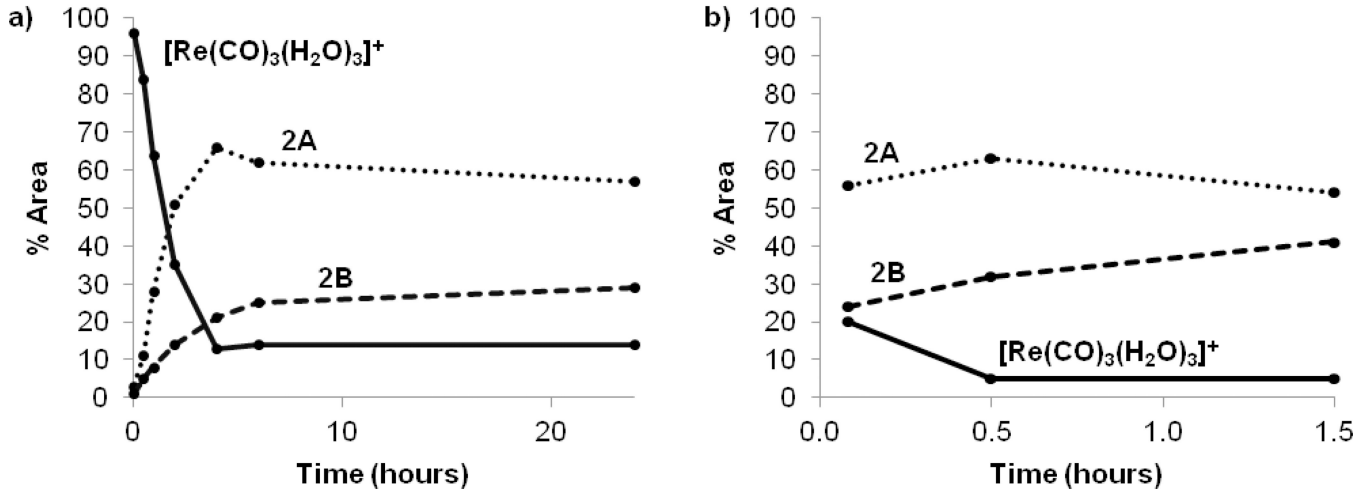

Figure 3.

The progression of the major species formed and present in the reaction mixture (pH 6) of *L*-ASMA, **1**, with a slight excess of $[Re(CO)_3(H_2O)_3]^+$ as assessed by the relative % area of HPLC traces. Increasing the reaction temperature from 20 °C (a) to 70 °C (b) significantly accelerated the reaction.

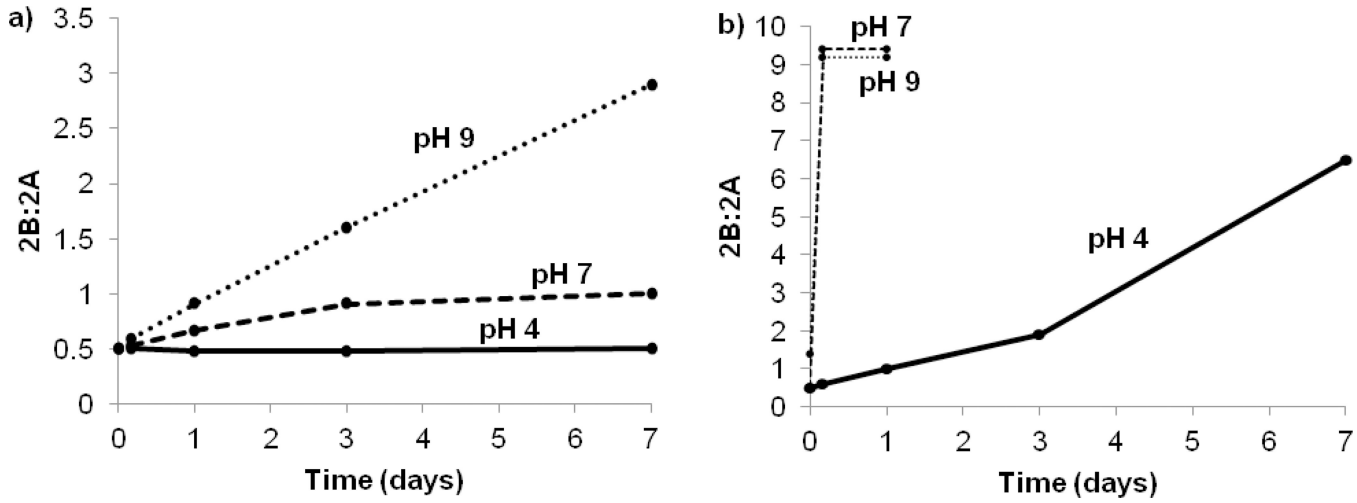

Figure 4.

The initial reaction for 1 d at 20 °C and pH 6 yielded a mixture of two $Re(CO)_3(\iota\text{-ASMA})$ isomers, **2A** (exo) and **2B** (endo). The product ratio of the crude reaction mixture was studied by monitoring the % area from the HPLC trace for up to 7 d at 20 °C (a) and 70 °C (b) for pH 4, 7 and 9.

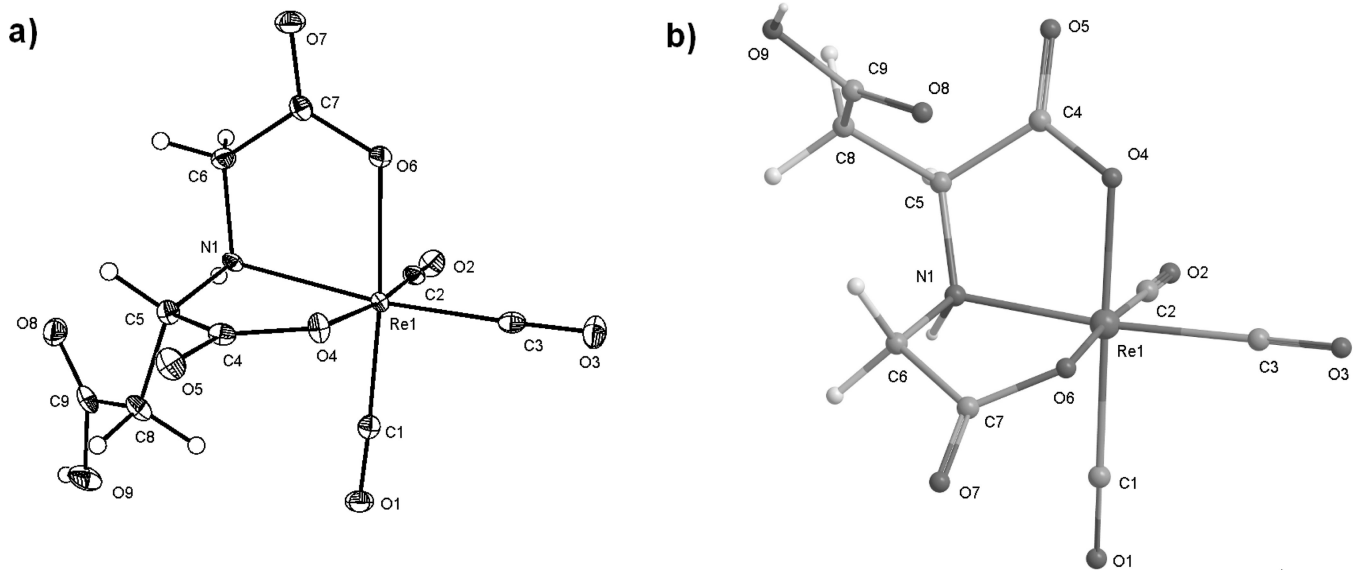

Figure 5.

(a) ORTEP representation of one enantiomer (from *L*-ASMA) of the anion of K[*endo*-$Re(CO)_3$(*rac*-ASMA)], **2B**. Hydrogen atoms are shown in their calculated positions. The K^+ cation is omitted for clarity. (b) A model of *exo*-$Re(CO)_3$(*L*-ASMA) (**2A**) calculated using the MM2 force field[18] to illustrate the exo orientation of the dangling acetate group.

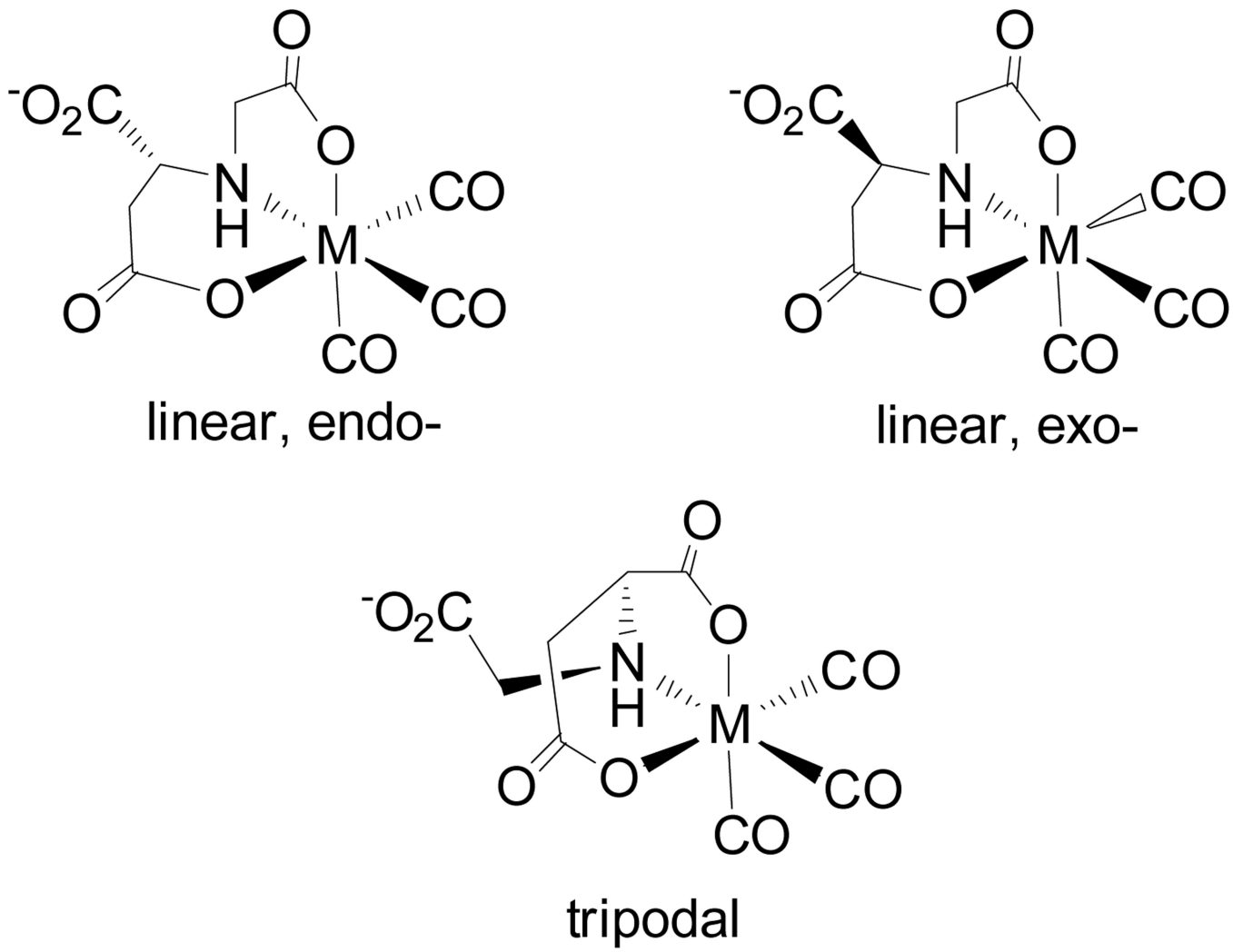

Figure 6.

Conceivable isomers of $Re(CO)_3$(ASMA) with the β-carboxyl group coordinated to the metal core. Enantiomers of the isomers shown would also exist, but are not pictured. For clarity, the complexes are shown without formal charges or counterions. Linearly coordinated isomers contain adjacent five- and six-membered chelate rings, whereas tripodal isomers contain a seven-membered ring.

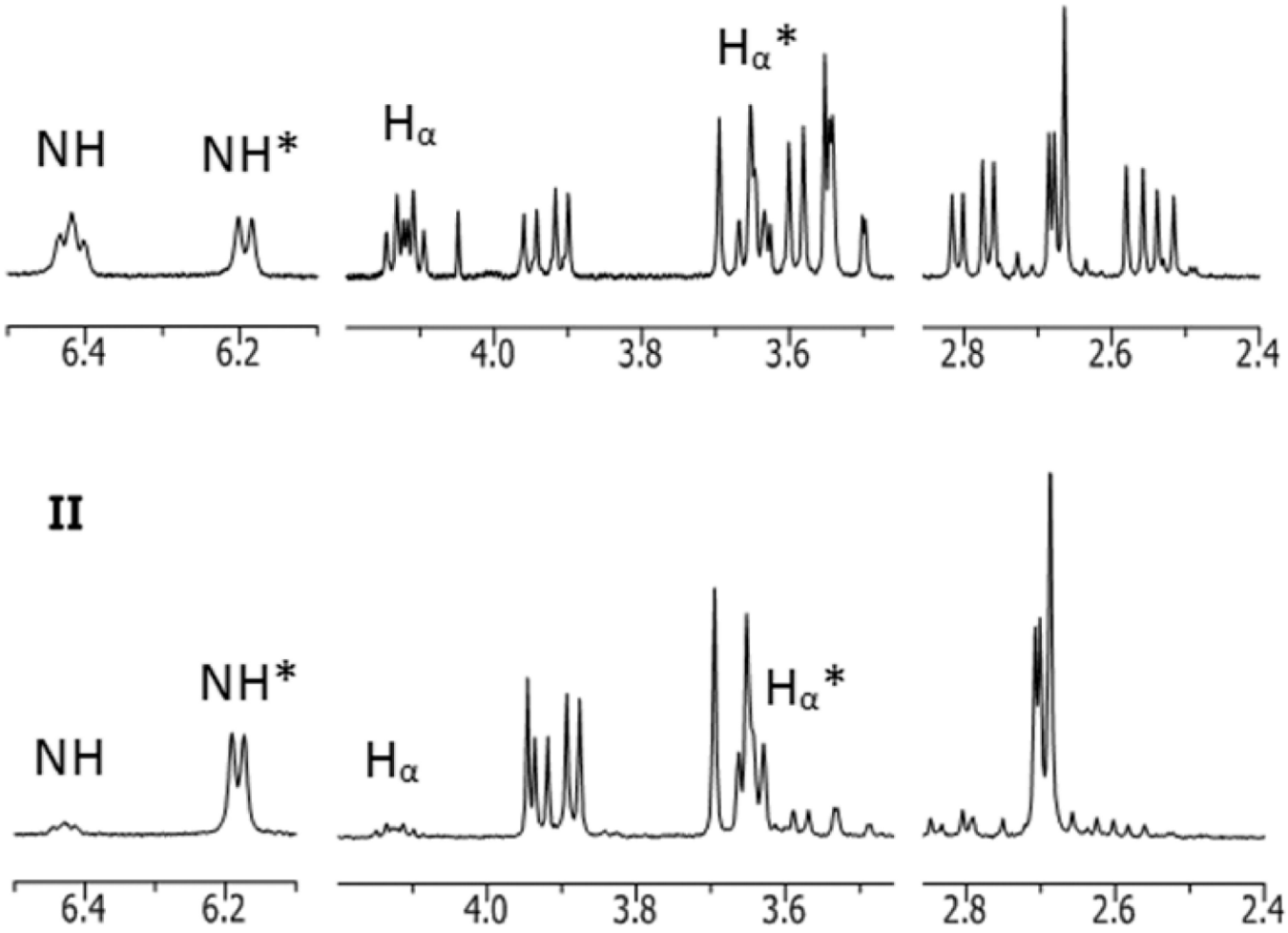

Figure 7.

^{1}H NMR spectra (D_2O, 20 °C, pH 6) of $Re(CO)_3$(*L*-ASMA) maintained at 20 °C (**I**) and after heating at 70 °C for 3 d (**II**) are shown (detailed in Table 2). The signals from *exo*-$Re(CO)_3$(*L*-ASMA) (**2A**) and *endo*-$Re(CO)_3$(*L*-ASMA) (**2B**) can be deconvoluted by comparing the two spectra. Selected signals from **2A** (**I**) and **2B** (**II**, marked with an *) are labeled to highlight significant differences.

Table 1

Selected bond lengths (Å) and angles (°) for Re^{I} tricarbonyl complexes with ASMA and CMSA.[a]

K[*endo*-Re(CO)$_3$(*rac*-ASMA)]		NMe$_4$[*endo*-Re(CO)$_3$(CMSA)][9d]	
Distances			
Re1-C1	1.889(4)	Re1-C3	1.897(4)
Re1-C2	1.906(4)	Re1-C1	1.913(4)
Re1-C3	1.914(4)	Re1-C2	1.927(4)
Re1-O4	2.135(2)	Re1-O6	2.127(2)
Re1-N1	2.201(3)	Re1-S1	2.452(1)
Re1-O6	2.138(2)	Re1-O4	2.164(2)
C7-C9[b]	5.466	C4-C9[b]	5.824
C4-C9[b]	3.842	C6-C9[b]	3.005
Angles			
C1-Re1-N1	98.43(13)	C3-Re1-S1	95.86(11)
C1-Re1-C2	88.20(15)	C3-Re1-C1	89.23(14)
C1-Re1-C3	90.03(15)	C3-Re1-C2	88.30(15)
C1-Re1-O4	93.91(13)	C3-Re1-O6	95.92(12)
C2-Re1-N1	97.62(13)	C1-Re1-S1	94.89(12)
C2-Re1-O6	96.54(12)	C1-Re1-O4	90.78(11)
C2-Re1-C3	88.75(15)	C1-Re1-C2	91.17(16)
C3-Re1-O6	93.58(12)	C2-Re1-O4	95.92(12)
C3-Re1-O4	97.89(12)	C2-Re1-O6	93.33(13)
O6-Re1-N1	75.50((10)	O4-Re1-S1	79.94(6)
O6-Re1-N1	77.51(10)	O6-Re1-S1	80.29(7)
O4-Re1-O6	80.97(10)	O4-Re1-O6	83.76(8)
C2-Re1-O4	173.02(12)	C1-Re1-O6	173.25(12)
C1-Re1-O6	174.09(12)	C3-Re1-O4	175.78(13)
C3-Re1-N1	169.54(12)	C2-Re1-S1	172.69(12)

[a] Although the atom labels of each complex are inconsistent (labeled according to the appropriate CCDC file), each row lists an analogous length or angle.

[b] Nonbonded distances between carboxyl group carbons.

Table 2

^{1}H NMR data (D_2O, pH 6) for **2A** (exo) and **2B** (endo) isomers of the $[Re(CO)_3(L\text{-ASMA})]^{2-}$ anion.

^{1}H Signal	2A (exo)	2B (endo)
NH	6.42 (m, 1H)	6.18 (d, 1H, *J*=6.8 Hz)
H_α	4.12 (m, 1H, *J*=5.6, 8.8 Hz)	3.63 (dd, 1H, *J*=6.0, 8.0 Hz)
H_β	2.79 (dd, 1H, *J*=5.6,16.4 Hz)	2.70 (d, 2H, *J*=6.0 Hz)
	2.55 (dd, 1H, *J*=8.8,16.4 Hz)	2.70 (d, 2H, *J*=8.0 Hz)
exo-H_{COORD};	3.58 (m, 2H)	3.93 (dd, 1H, *J*=6.8, 17.2 Hz)
endo-H_{COORD}		3.67 (d, 1H, *J*=17.2 Hz)

Table 3

Comparison of ^{1}H NMR shifts (ppm) of exo- and endo- proton signals in various Re^{I} tricarbonyl complexes. Endo- protons are generally deshielded compared to analogous exo- protons.

Compound	^{1}H Signal	endo	exo
$Re(CO)_3$(ASMA)	H_α	4.12	3.63
endo-$Re(CO)_3$(ASMA)	H_{COORD}	3.93	3.67
$Re(CO)_3$(CMSA)[a]	H_α	3.97	3.50
$Re(CO)_3$(CCM)[b]	H_α	3.49	3.23
$Re(CO)_3$(ENDAC)[c]	N-H	5.45	5.03
$Re(CO)_3$(DTA)[d]	N-H	5.75	5.17

[a] CMSA[9d] = carboxymethylmercaptosuccinic acid

[b] CCM[8] = *S*-(carboxymethyl)-*L*-cysteine.

[c] ENDAC[9c] = ethylenediamine-*N,N′*-diacetic acid.

[d] DTA[9b] = diethylenetriamine-*N*-acetic acid.

Table 4

Additional details of the data collection and structure refinement of K[*endo*-Re(CO)$_3$(*rac*-ASMA)].

	2B and 4B
empirical formula	$C_9H_7KNO_9Re$
formula weight	498.46
T (K)	173 (2)
λ (Å)	0.71073
crystal system	monoclinic
space group	$P2_1/c$
unit cell dimensions	
a (Å)	7.952 (4)
b (Å)	14.774 (7)
c (Å)	10.879 (5)
β (deg)	98.417 (7)
V (Å3)	1264.4 (10)
Z	4
ρ_{calc} (mg/m^3)	2.619
abs coeff (mm^{-1})	9.988
R indices [$I > 2\sigma(I)$]	$R_1 = 0.0260$
	w$R_2 = 0.0590$